PLOS ONE

RESEARCH ARTICLE

Glioma Cells in the Tumor Periphery Have a Stem Cell Phenotype

Sune Munthe[1,2,3]*, Stine Asferg Petterson[1], Rikke Hedegaard Dahlrot[4], Frantz Rom Poulsen[2,3], Steinbjørn Hansen[2,4], Bjarne Winther Kristensen[1,2]

1 Department of Pathology, Odense University Hospital, 5000 Odense C, Denmark, **2** Institute of Clinical Research, University of Southern Denmark, 5000 Odense C, Denmark, **3** Department of Neurosurgery, Odense University Hospital, 5000 Odense C, Denmark, **4** Department of Oncology, Odense University Hospital, 5000 Odense C, Denmark

* sune.munthe@rsyd.dk

Citation: Munthe S, Petterson SA, Dahlrot RH, Poulsen FR, Hansen S, Kristensen BW (2016) Glioma Cells in the Tumor Periphery Have a Stem Cell Phenotype. PLoS ONE 11(5): e0155106. doi:10.1371/journal.pone.0155106

Editor: Maria G Castro, University of Michigan School of Medicine, UNITED STATES

Received: November 16, 2015

Accepted: April 25, 2016

Published: May 12, 2016

Data Availability Statement: Data are available from Figshare (https://figshare.com/s/939a79008964ca53bfc1).

Funding: The authors have no support or funding to report.

Competing Interests: The authors have declared that no competing interests exist.

Abstract

Gliomas are highly infiltrative tumors incurable with surgery. Although surgery removes the bulk tumor, tumor cells in the periphery are left behind resulting in tumor relapses. The aim of the present study was to characterize the phenotype of tumor cells in the periphery focusing on tumor stemness, proliferation and chemo-resistance. This was investigated in situ in patient glioma tissue as well as in orthotopic glioblastoma xenografts. We identified 26 gliomas having the R132 mutation in Isocitrate DeHydrogenase 1 (mIDH1). A double immunofluorescence approach identifying mIDH1 positive tumor cells and a panel of markers was used. The panel comprised of six stem cell-related markers (CD133, Musashi-1, Bmi-1, Sox-2, Nestin and Glut-3), a proliferation marker (Ki-67) as well as a chemo-resistance marker (MGMT). Computer-based automated classifiers were designed to measure the mIDH1 positive nucleus area-fraction of the chosen markers. Moreover, orthotopic glioblastoma xenografts from five different patient-derived spheroid cultures were obtained and the tumor cells identified by human specific immunohistochemical markers. The results showed that tumor cells in the periphery of patient gliomas expressed stem cell markers, however for most markers at a significantly lower level than in the tumor core. The Ki-67 level was slightly reduced in the periphery, whereas the MGMT level was similar. In orthotopic glioblastoma xenografts all markers showed similar levels in the core and periphery. In conclusion tumor cells in the periphery of patient gliomas have a stem cell phenotype, although it is less pronounced than in the tumor core. Novel therapies aiming at preventing recurrence should therefore take tumor stemness into account. Migrating cells in orthotopic glioblastoma xenografts preserve expression and stem cell markers. The orthotopic model therefore has a promising translational potential.

Introduction

Treatment of gliomas is a major challenge. Despite treatment consisting of surgery, chemotherapy and radiation the mean survival of patients with the most common and malignant primary

brain tumor, the WHO grade IV Glioblastoma multiforme (GBM), is approximately 14.6 months [1]. A major challenge in treatment of gliomas is the high migratory potential of glioma cells [2]. Migrating glioma cells are not eligible to surgery and therefore eradication by radiation and chemotherapy is standard strategy.

The high resistance of gliomas against conventional radiation and chemotherapy has been suggested to be due to the existence of immature cancer stem cells (CSC), which are tumor cells with a stem cell-like phenotype sustaining glioma growth through asymmetric cell division [3, 4]. These cells have been suggested to be resistant towards conventional treatment due to enhanced DNA repair and enhanced expression of ATP-binding cassette drug transporters [5]. The presence of CSCs in the periphery of gliomas has not previously been thoroughly investigated. We therefore hypothesized that migrating glioma cells display a stem cell phenotype and express stem cell markers. Since proliferation and chemo-resistance are important determinants for the effect of radiation and chemotherapy, the markers Ki-67 and MGMT were included. The aim of this study was to characterize the expression of stem cell markers as well as markers of proliferation and chemo-resistance in migrating glioma cells by using a double immunofluorescence approach on patient glioma tissue and GBM xenografts.

In patient tumor tissue a mutated form of Isocitrate dehydrogenase 1 (mIDH1) [6] was used as a tumor cell specific marker. The somatic point mutation that affects codon 132 is the most frequent IDH1 mutation and a specific well described antibody recognizing mIDH1 R132 has recently been developed [7, 8]. This mutation is primarily associated with grade II and III gliomas but is also found in secondary GBMs [9].

In glioma research the most preferred *in vivo* model is the orthotopic xenograft model. Here GBM cells are implanted into the brain of immunosuppressed animals. The model is well established in our laboratory and has been described by several groups [10, 11]. Using this model together with a double immunofluorescence approach and human specific markers to identify the tumor cells, the marker expression in migrating glioma cells was characterized. For this characterization a panel of markers similar to that used for patient gliomas was used.

We have previously used fluorescence for quantification of biomarkers in gliomas [12]. In this study we combined the tumor cell specific markers in a double immunofluorescence protocol with the following panel of stem cell markers: CD133 [4, 13–18], Nestin [18–24], Musashi-1 [18, 25–28], Sox-2 [18, 29–32] and Bmi-1 [18, 29, 32, 33], to characterize the phenotype of migrating glioma cells. We also investigated the glucose transporter type III (Glut-3) in the core and periphery since it has been reported to be associated with stemness [34]. Furthermore, we investigated the expression of the DNA repair enzyme O^6-methylguanine-DNA methyltransferase (MGMT) in the core of the tumor and compared it to the periphery, since MGMT is a strong prognostic and predictive marker for the effect of temozolomide in the upfront GBM treatment [35]. The proliferation of migrating tumor cells has previously been investigated by Sabit *et al.* [36] who investigated 11 patients. We wanted to futher explore this in our cohort consisting of 26 patients as well as by using the orthotopic GBM xenograft model.

Material and Methods

Patient selection and pathology

Adult residents in the Region of Southern Denmark diagnosed with primary brain cancer between 1st of January 2005 and 31st of December 2009 were identified in the Danish Cancer Register (DCR). Patients with the histopathological codes for gliomas (M 94003, M 94013, M 94403, M 94503, M 94513, M 93823, and M 93853) were considered for inclusion in the present study, giving a total of 277 patients. The mIDH1 status was identified by immunohistochemical staining; 47 patients were mIDH1 positive. Twenty six patients were identified with

Table 1. Summary of patients.

Histopathological diagnosis	Number of mIDH1 patients	Age (years)		WHO grade
		Median	Range	
diffuse astrocytoma	6 (23.1%)	41	30–62	II
oligodendroglioma	7 (26.9%)	48.9	31–81	II
oligoastrocytoma	5 (19.2%)	46.8	26–74	II
anaplastic astrocytoma	2 (7.7%)	46	34–58	III
anaplastic oligodendroglioma	1 (3.8%)	38	38	III
anaplastic oligoastrocytoma	2 (7.7%)	41	36–46	III
glioblastoma	3 (11.5 %)	60.3	43–75	IV
Total	26	46.7	26–81	

doi:10.1371/journal.pone.0155106.t001

both a tumor core and a periphery zone present in the same tumor section. The different mIDH1 positive gliomas are listed according to the WHO classification in Table 1. The histopathological evaluation was carried out at the Department of Pathology at Odense University Hospital. All tissue samples were evaluated by two pathologists and classified according to WHO guidelines 2007 [37].

Xenograft model

For establishing the orthotopic xenograft model we used 5 different GBM spheroid cultures, established in our laboratory from patient-derived GBM tumor tissue, collected at the Department of Neurosurgery, Odense University Hospital. Tumor cells were grown and stem cell phenotypes validated as previously described in our laboratory [38]. The five GBM spheroid cultures were named: T78, T86, T87, T111 and T113.

Female Balb c nu/nu mice 7–8 weeks of age were anesthetized subcutaneously with injection of a mixture of Hypnorm and Dormicum (0,1ml/10g). The mice were placed in a stereotactic frame (Model 900, David Kopf Instrument). A midline incision was made exposing bregma and a burr hole was made 1 mm anterior and 2 mm lateral to bregma. A syringe (2 μl Hamilton syringe) with a blunt needle containing 150.000 cells/μl was inserted 3 mm into the brain and 2 μl were injected slowly into the brain over several minutes. The needle was slowly removed to prevent a vacuum causing the tumor cells to escape. The skin was sutured with resorbable sutures. If the mice showed any signs of neurological deficit or weight loss more than 20%, the mice were euthanized in a carbon dioxide chamber. The brains were immediately removed and fixated in 4% formalin for 48 hours. Before paraffin embedding the brains were manually divided by 1mm coronal sections. Histological sections were afterwards cut and immunohistochemically stained with Vimentin, a human specific antibody. In mice implanted with the GBM spheroid culture T86 CD56, another human specific antibody, was used for identification of the tumor cells. The GBM spheroid cultures T86 and T113 were found to have unmethylated MGMT promoter, whereas the remaining GBM spheroid cultures were methylated in the promoter region. We therefore did not investigate the MGMT in the *in vivo* model. We defined the core in our *in vivo* model as striatum and the periphery as corpus callosum in the contra lateral side.

Immunohistochemical staining

Histological sections of three μm were cut on a microtome and placed on glass slides. Tissue was deparaffinized, and antigen retrieval was carried out in a microwave oven using the Tris

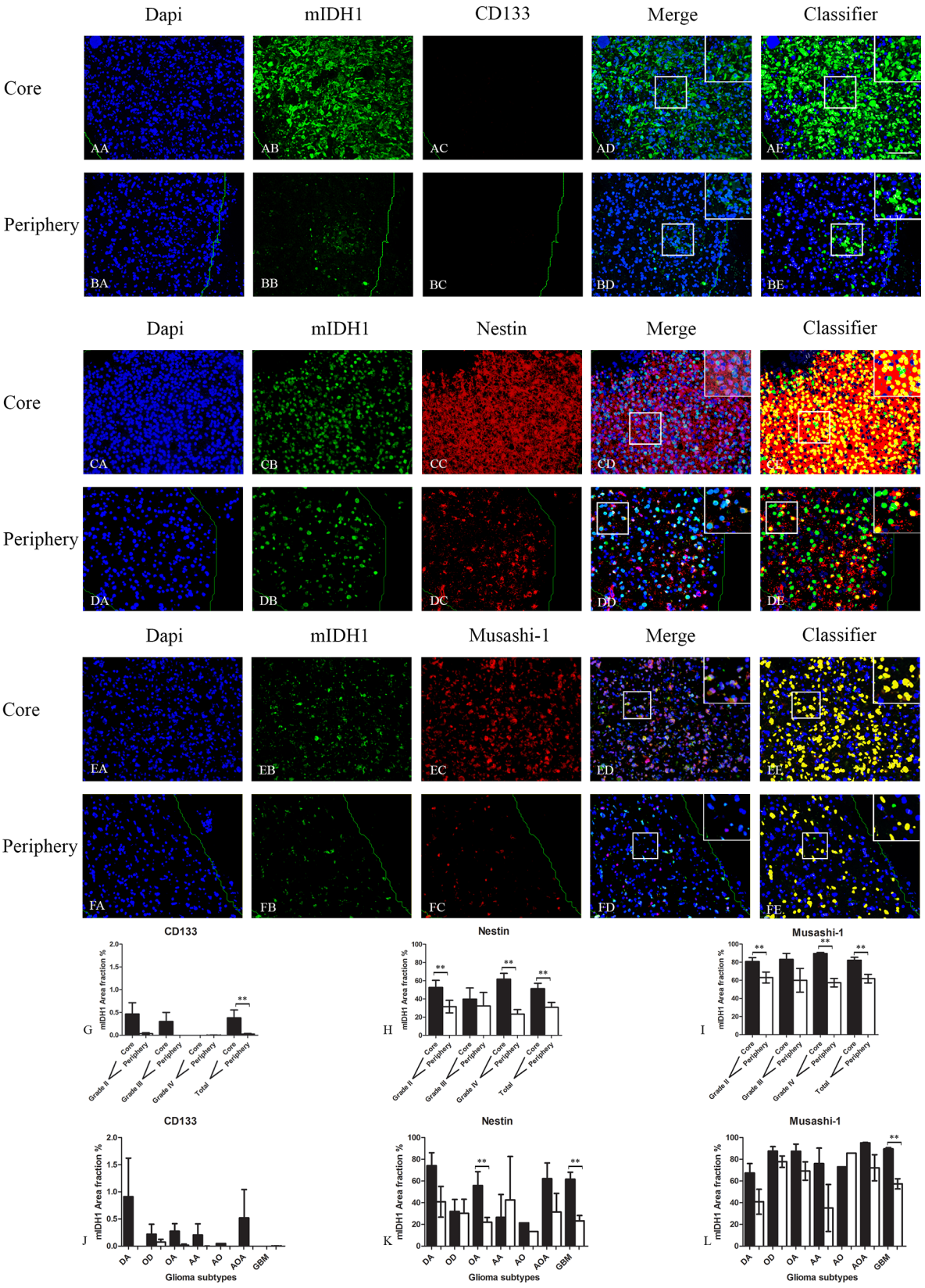
Dapi
mIDH1
CD133
Merge
Classifier
Core
Periphery
AA
AB
AC
AD
AE
BA
BB
BC
BD
BE
Dapi
mIDH1
Nestin
Merge
Classifier
Core
Periphery
CA
CB
CC
CD
CE
DA
DB
DC
DD
DE
Dapi
mIDH1
Musashi-1
Merge
Classifier
Core
Periphery
EA
EB
EC
ED
EE
FA
FB
FC
FD
FE
CD133
Nestin
Musashi-1
G
H
I
mIDH1 Area fraction %
Core
Periphery
Grade II
Grade III
Grade IV
Total
CD133
Nestin
Musashi-1
J
K
L
mIDH1 Area fraction %
DA
OD
OA
AA
AO
AOA
GBM
Glioma subtypes

Fig 1. Double immunofluorescence staining of core and periphery of patient glioblastomas. Histological sections were stained with Dapi (blue), IDH1 (green) and CD133 (red) (AA-BE), Nestin (red) (CA-DE) and Musashi-1 (red) (EA to FE). The software-based classifier is shown in the right column. The classifier illustrates tumor cells co-expressing markers of interest in yellow and tumor cells not co-expressing markers of interest in green. The fluorescence stainings were quantified in both core and periphery for CD133 (G,J), Nestin (H,K) and Musashi-1 (I,L). Statistical comparison was performed using student's t-test and ANOVA, ** p< 0.01. Scalebar: 200μm.

doi:10.1371/journal.pone.0155106.g001

EGTA buffer. Slides were stained on the AutostainerPlus platform (DAKO, Glostrup, Denmark). For mIDH1 staining slides were incubated with antibody (mIDH1 R132H, Clone H09, Dianova, 1:100) and the detection system ultraViewTM Universal DAB Detection Kit (Ventana Medical Systems) was subsequently used. For each patient, tumor slide was stained by a double immuno-fluorescence approach combining mIDH1 and 6 different stem cell-related markers: CD133 (clone: W6B3C1, Miltenyi Biotec), Musashi-1 (clone:14H1, MBL International), Bmi-1 (clone: F6, Upstate Cell Signaling Solution), Sox-2 (clone: 245610, R&D Systems Inc.), Nestin (clone: 196908, R&D Systems Inc.), Glut-3 (clone: HPA006539, Atlas Antibodies), MGMT (clone: MT23.2, Invitrogen) and the proliferation marker Ki-67 (clone: MIB1, Beckman Coulter). The CSA II Biotin-free Tyramide signal Amplification System kit (DAKO) was used for detection of mIDH1 (1+1600). Detection of the second antibody was performed using a Tyramide Signal Amplification (TSA) Plus System with Cyanin 5 (Cy5); CD133 (1+40), Musashi (1+200), Bmi-1 (1+200), Sox-2 (1+400), Nestin (1+200), GLUT-3 (1+100), MGMT (1+100) and Ki67 (1+800). The nuclei were counterstained with 4´,6 diamidino-2-phemylindole (Dapi) (VWR Internation ApS).

For each xenograft slide a double immuno-fluorescence staining with Vimentin and the same six stem cell markers and Ki-67 was made. For xenograft slides with T86 tumors, CD56 was used as a tumor marker since it was Vimentin negative. The Alexa Flour-488 donkey anti-rabbit (1+100) was used to detect Vimentin (1+400, EP20, Epitomics) and CSA II Biotin-free Tyramide signal Amplification System kit (DAKO) was used for detection of CD56 (1+3200, CO4-NCAM, Neomarkers) in the T86 tissue samples. The nuclei were counterstained with 4´.6 diamidino-2-phemylindole (Dapi) (VWR Internation ApS).

Automated Quantitative analysis

Super images of whole slides were taken at 1.25x magnification using a Leica DM6000 B microscope with an Olympus DP72 camera with bright field settings. Subsequently the region of interest (ROI), both the core and periphery, was manually outlined for each tumor section using the Visiopharm Integrator System (VIS) version: 4.5.6.440 (Visiopharm, Hørsholm, Denmark). Sampling was performed at 20x magnification with a minimum of 15 images in each ROI. Images were reviewed to ensure that no artifacts or blurring were present. Then images were analyzed using an algorithm developed in the Visiomorph software module. A specific classifier was developed for each double-fluorescence staining according to the Visiopharm Manual. Classifiers were designed and trained so nuclear area corresponding to DAPI staining of positive cells were measured. In each specific classifier we calculated the total area of the nuclei of tumor cells of interest (labeled by tumor cell specific marker and marker of interest) and the total area of remaining tumor cell nuclei (labeled by tumor cell specific marker but not by marker of interest). From these areas, the nuclear area fraction of tumor cells labeled by marker of interest was calculated in core and periphery. This fraction was determined based on the whole mIDH1 positive cell population in each ROI. It was not determined on a single cell basis, since core areas with very high cellularity did not allow complete separation of the DAPI stained nuclei.

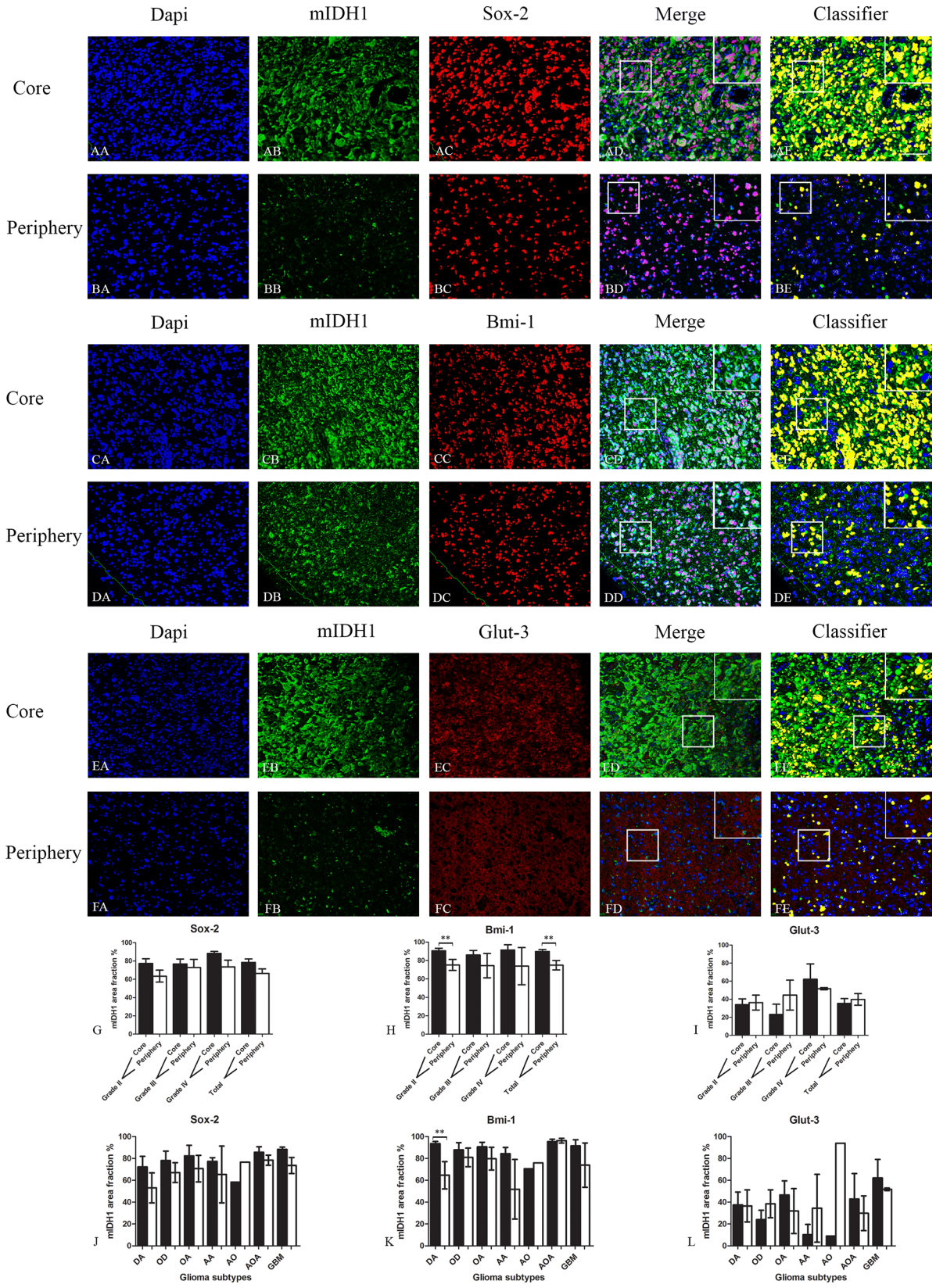
Dapi
mIDH1
Sox-2
Merge
Classifier
Core
Periphery
AA
AB
AC
AD
AE
BA
BB
BC
BD
BE
Dapi
mIDH1
Bmi-1
Merge
Classifier
Core
Periphery
CA
CB
CC
CD
CE
DA
DB
DC
DD
DE
Dapi
mIDH1
Glut-3
Merge
Classifier
Core
Periphery
EA
EB
EC
ED
EE
FA
FB
FC
FD
FE
Sox-2
Bmi-1
Glut-3
mIDH1 area fraction %
Grade II
Grade III
Grade IV
Total
G
H
I
J
K
L
DA
OD
OA
AA
AO
AOA
GBM
Glioma subtypes

Fig 2. Double immunofluorescence staining of core and periphery of patient glioblastomas. Histological sections were stained with Dapi (blue), IDH1 (green) and Sox-2 (red) (AA-BE), Bmi-1 (red) (CA-DE) and Glut-3 (red) (EA to FE). The software-based classifier is shown in the right column. The classifier illustrates tumor cells co-expressing markers of interest in yellow and tumor cells not co-expressing markers of interest in green. The fluorescence stainings were quantified in both core and periphery for Sox-2 (G,J), Bmi-1 (H,K) and Glut-3 (I,L). Statistical comparison was performed using student's t-test and ANOVA, ** $p< 0.01$. Scalebar: 200μm.

doi:10.1371/journal.pone.0155106.g002

Statistics

Data was analyzed in GraphPad Prism version 5.01. The comparison of area fraction in the core and periphery was performed with an unpaired t-test. Statistical significance was defined as $p < 0.05$.

Ethics

The official Danish ethical review board named the Regional Scientific Ethical Committee of the Region of Southern Demark approved the use of human glioma tissue (permission J. No. S-2011 0022) in the current study. Written informant consent was obtained from all participants. The use of animals in the present study was approved by The Animal Experiment Inspectorate in Denmark (J. Nr. 2013/15-2934-00973).

Results

CD133 expression was significantly reduced in migrating tumor cells in the tumor periphery compared to tumor cells in the core region when comparing levels in all tumor samples. Similar but not significant results were obtained in the different grades and glioma subtypes (Fig 1G and 1J).

Nestin expression was significantly reduced in the periphery for tumor grade II and IV and for all gliomas together (Fig 1H). For the different glioma subtypes only Oligo-Astrocytoma (OA) and GBM revealed significantly reduced expression in the periphery although the same trend was found in the other subtypes (Fig 1K).

The expression of Musashi-1 was significantly reduced in the periphery for grade II and IV and in all gliomas together (Fig 1I). For the different subtypes of gliomas only GBM had a reduced expression in the periphery, although the same trend was found in the other subtypes (Fig 1L).

The expression of Sox-2 was reduced in the periphery for all tumor grades and subtypes (S1 Fig) except for the Anaplastic Oligodendroglioma (AO), but without reaching significance (Fig 2G and 2J).

The expression of Bmi-1 was significantly reduced in the periphery of grade II tumors and all gliomas together (Fig 2H). For subtypes, only the Diffuse Astrocytoma (DA) had a significantly reduced expression in the periphery. The expression of Bmi-1 was reduced in the periphery of all subtypes except the Anaplastic Oligodendroglioma (AO), but without reaching significance (Fig 2K).

Glut-3 expression was apparently expressed at similar levels in core and periphery (Fig 2I and 2L).

The expression of Ki-67 was significantly reduced in the periphery for all gliomas together (Fig 3E). Similar but no significantly reduced expression of Ki-67 in periphery compared to core was obtained in the different grades and glioma subtypes (Fig 3E and 3G).

MGMT was expressed at similar levels in core and periphery (Fig 3F and 3H).

Comparing expression of the different markers between grades, we did observe a significant increase in the Ki-67 expression in the core area from grade II to grade IV (Fig 3E). There was no significant increase of expression of other markers with grade.

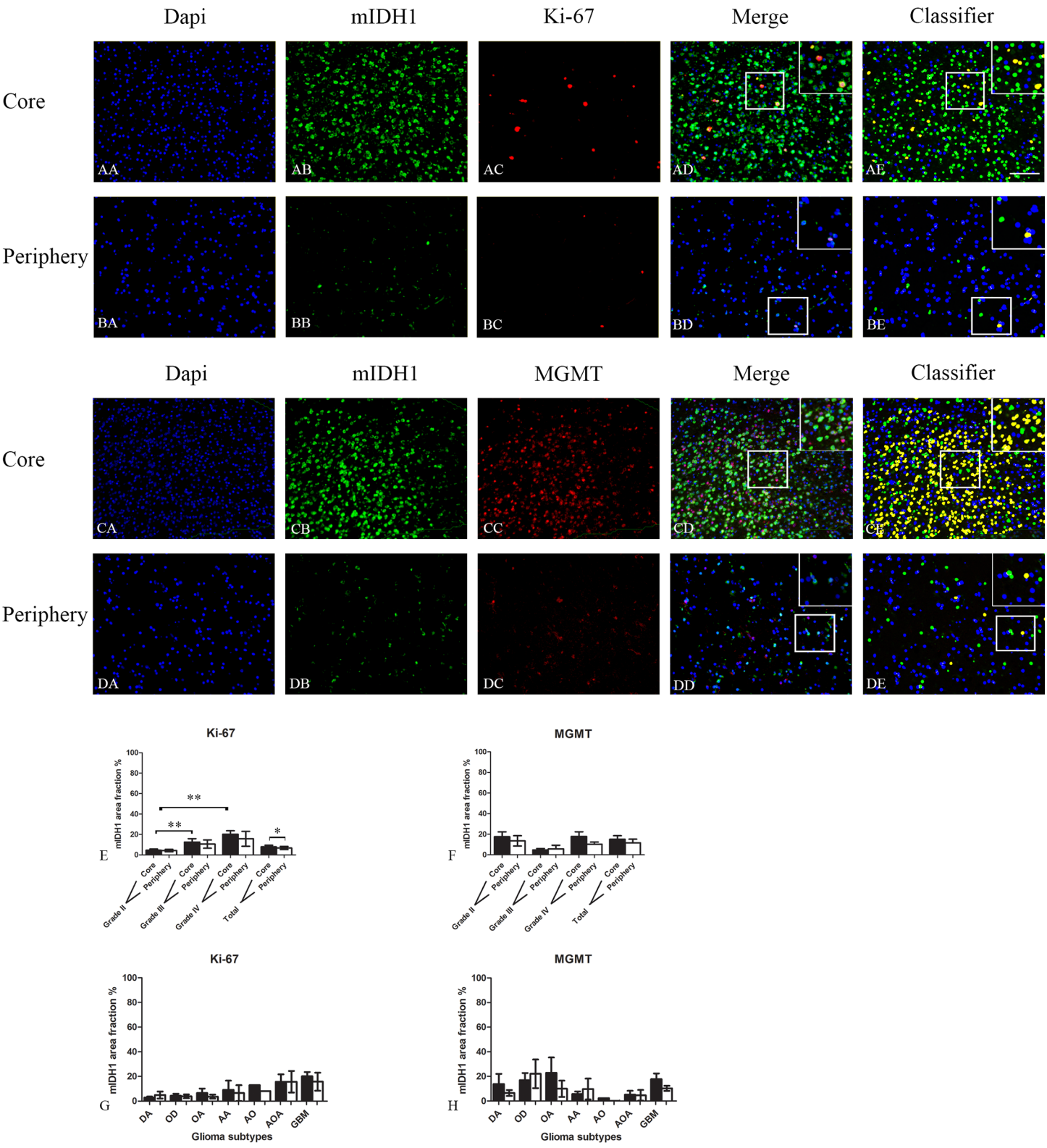

Fig 3. Double immunofluorescence staining of core and periphery of patient gliomas. Two glioblastomas (AA-BE and CA-DE) were stained with Dapi (blue), IDH1 (green) and Ki-67 (red) and MGMT (red). The software-based classifier is shown in the right column. The classifier illustrates tumor cells co-expressing markers of interest in yellow and tumor cells not co-expressing markers of interest in green. The fluorescence stainings were quantified in both core and periphery for Ki-67 (E,G) and MGMT (F,H). Statistical comparison was performed using student's t-test and ANOVA, ** p< 0.01. Scalebar: 200μm.

doi:10.1371/journal.pone.0155106.g003

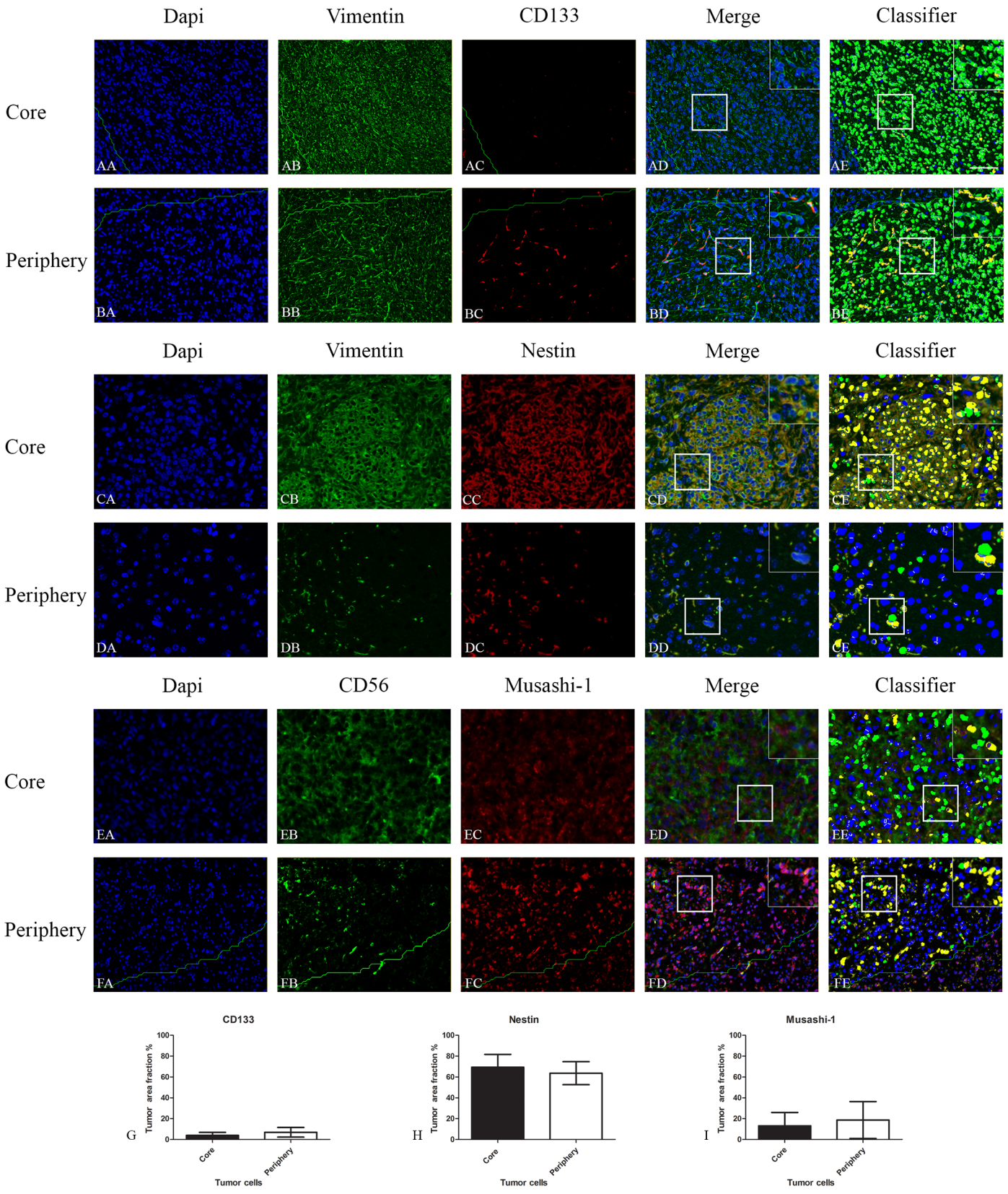
Dapi
Vimentin
CD133
Merge
Classifier
Core
Periphery
AA
AB
AC
AD
AE
BA
BB
BC
BD
BE
Dapi
Vimentin
Nestin
Merge
Classifier
Core
Periphery
CA
CB
CC
CD
CE
DA
DB
DC
DD
CE
Dapi
CD56
Musashi-1
Merge
Classifier
Core
Periphery
EA
EB
EC
ED
EE
FA
FB
FC
FD
FE
G
CD133
Tumor area fraction %
100
80
60
40
20
0
Core
Periphery
Tumor cells
H
Nestin
Tumor area fraction %
100
80
60
40
20
0
Core
Periphery
Tumor cells
I
Musashi-1
Tumor area fraction %
100
80
60
40
20
0
Core
Periphery
Tumor cells

Fig 4. Double immunofluorescence staining of core and periphery in orthotopic model with five different patient-derived GBM spheroid cultures. Tissues were stained with Dapi (blue), Vimentin/CD56 (green) and CD133 (red), Nestin (red) and Musashi-1 (red). The software-based classifier is shown in the right column. The classifier illustrates tumor cells co-expressing markers of interest in yellow and tumor cells not co-expressing markers of interest in green. The fluorescence stainings were quantified in both core and periphery for CD133 (G), Nestin (H) and Musashi-1 (I). Statistical comparison was performed using student's t-test. Scalebar: 200μm.

doi:10.1371/journal.pone.0155106.g004

In the GBM xenografts the different markers were expressed at similar levels in core and periphery (Figs 4, 5 and 6).

Discussion

Our results suggest that tumor cells in the periphery express CSC-markers both in patient gliomas and in orthotopic xenografts. The CSC hypothesis states that tumor growth is driven by a subpopulation of tumorigenic CSCs [39]. Huang *et al*. and Bao *et al*. showed that CSCs in GBMs were extremely resistant to conventional radiation and chemotherapies [3, 40]. Together these results suggest that the CSC hypothesis also extend to tumor cells left in the periphery after surgery, although the vast majority of studies have been performed on removed central tumor material. The presence of CSCs in the periphery in all glioma grades and sub-types indicates that these CSCs could be the reason for treatment failure and recurrence in glioma patients. Extending the CSC hypothesis to tumor cells left in the periphery after surgery for all gliomas is fully in line with the well know observation that macro radical resection of the tumors increases survival compared to biopsies and suboptimal resection [41, 42].

Expression of CD133 was found at lower level compared to the other stem cell markers. This observation corresponds to what has been shown in other studies [43]. We have previously shown that it is of great importance which CD133 clone is used; e.g. whether the CD133 clone targets the non-glycosylated epitope (i.e. the C24B9 clone) or the glycosylated extracellular epitope (i.e. the AC133 or W6B3C1)[44]. In this study we used the W6B3C1 clone, which we previously have identified as an antibody clone labeling both membrane and cytoplasm of tumor cells [44–46]. Most importantly this clone has been shown to be associated with asymmetric tumor cell division, which is a hallmark of cancer stem cells [44, 47].

For Ki-67, the expression was slightly reduced in the periphery for all gliomas together. Comparing the expression between grades, we did however observe a significant increase in the Ki-67 expression in the core area from grade II to grade IV (Fig 3E). There was no significant increase in expression of other markers together with tumor grade. This is in line with the results from Sabit *et al.* [36] who used a similar mIDH1 double fluorescence approach (11 patients). However Sabit *et al*. did not use a computer-based algorithm, but two independent neuropathologists to evaluate the tumor samples. The slightly reduced proliferation in the periphery suggest that both temozolomide and radiation therapy is less efficient in these areas compared to central tumor areas. This may explain why Ki-67 labeling indices found and used in prognostic studies, where tumor bulk is removed, not have shown to have a prognostic value predicted [48, 49]. In most patients, it is in fact the tumor periphery left in the patients, which receives temozolomide and radiation therapy.

The Ki-67 labeling index correlated with survival should ideally be the index obtained from the periphery.

For MGMT a similar distribution in the core and periphery was found for all tumor grades and subtypes. This means that resistance to temozolomide was preserved in migrating tumor cells. Strategies aiming at reducing chemoresistance by compromising the MGMT enzyme are therefore highly relevant for migrating glioma cells and new drugs added to temozolomide should also reach these tumor cells to be efficient.

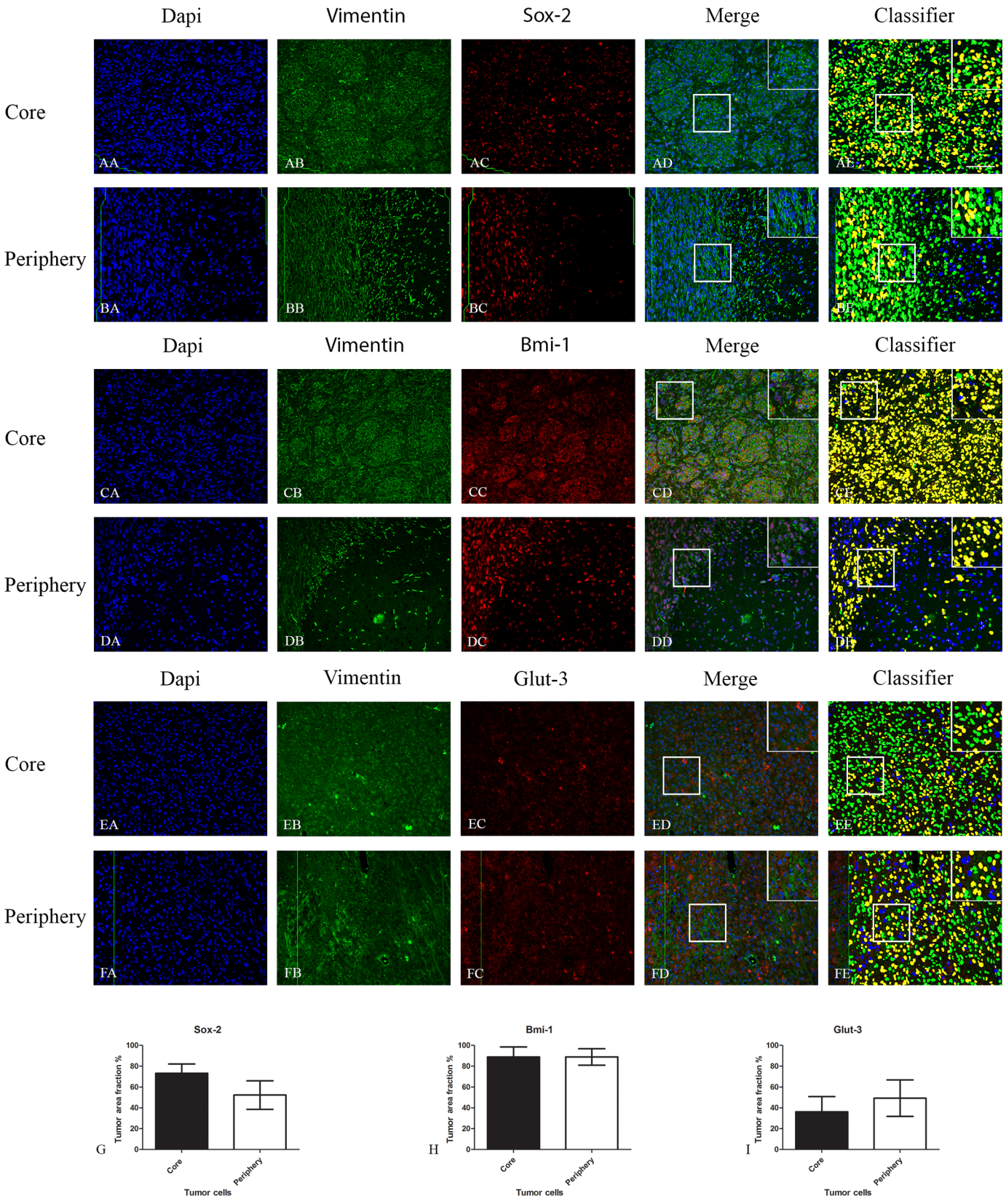
Dapi
Vimentin
Sox-2
Merge
Classifier
Core
Periphery
AA
AB
AC
AD
AE
BA
BB
BC
BD
BE
Dapi
Vimentin
Bmi-1
Merge
Classifier
Core
Periphery
CA
CB
CC
CD
CE
DA
DB
DC
DD
DE
Dapi
Vimentin
Glut-3
Merge
Classifier
Core
Periphery
EA
EB
EC
ED
EE
FA
FB
FC
FD
FE
G
Sox-2
Tumor area fraction %
Core
Periphery
Tumor cells
H
Bmi-1
Tumor area fraction %
Core
Periphery
Tumor cells
I
Glut-3
Tumor area fraction %
Core
Periphery
Tumor cells

Fig 5. Double immunofluorescence staining of core and periphery in orthotopic model with five different patient derived GBM spheroid cultures. Tissues were stained with Dapi (blue), Vimentin (green) and Sox-2 (red), Bmi-1 (red) and Glut-3 (red). The software-based classifier is shown in the right column. The classifier illustrates tumor cells co-expressing markers of interest in yellow and tumor cells not co-expressing markers of interest in green. The fluorescence stainings were quantified in both central part and periphery for Sox-2 (G), Bmi-1 (H) and Glut-3 (I). Statistical comparison was performed using student's t-test. Scalebar: 200μm.

doi:10.1371/journal.pone.0155106.g005

In the GBM xenograft mouse model the results showed a similar expression of stem cell markers in core and periphery for all stem cell markers. Before implantation in mice brains, the spheroid cultures were grown in neural stem cell medium, which favor a more stem cell like phenotype. This might explain the preservation of the stem cell phenotype in migrating xenograft tumor cells compared to the reduced expression of stem cell markers found in migrating glioma cells in patients. However, to a large extend the overall levels in tumor core in patients and mice were similar, except for musashi-1 and sox-2 which were expressed at much higher or higher levels in both core and periphery in patients GBMs compared to GBM xenografts. Reasons for this may be differences e.g. in tumor microenvironment. Hypoxia is pronounced in patient high grade gliomas and known to increase expression of stem cell markers [50–52], but necrosis is not found in our GBM xenografts suggesting that this micro-environmental stimulus is less pronounced patients. Another explanation of differences between results obtained in patient tumors versus GBM xenografts is IDH1 status. The patient tumors included in this study were all IDH1 mutated whereas all GBM xenografts were obtained from IDH1 wild type GBMs. Accordingly, CD133 has been found to be expressed at higher levels in IDH1 wild type GBMs compared to IDH1 mutated GBMs [53]. However, another marker of

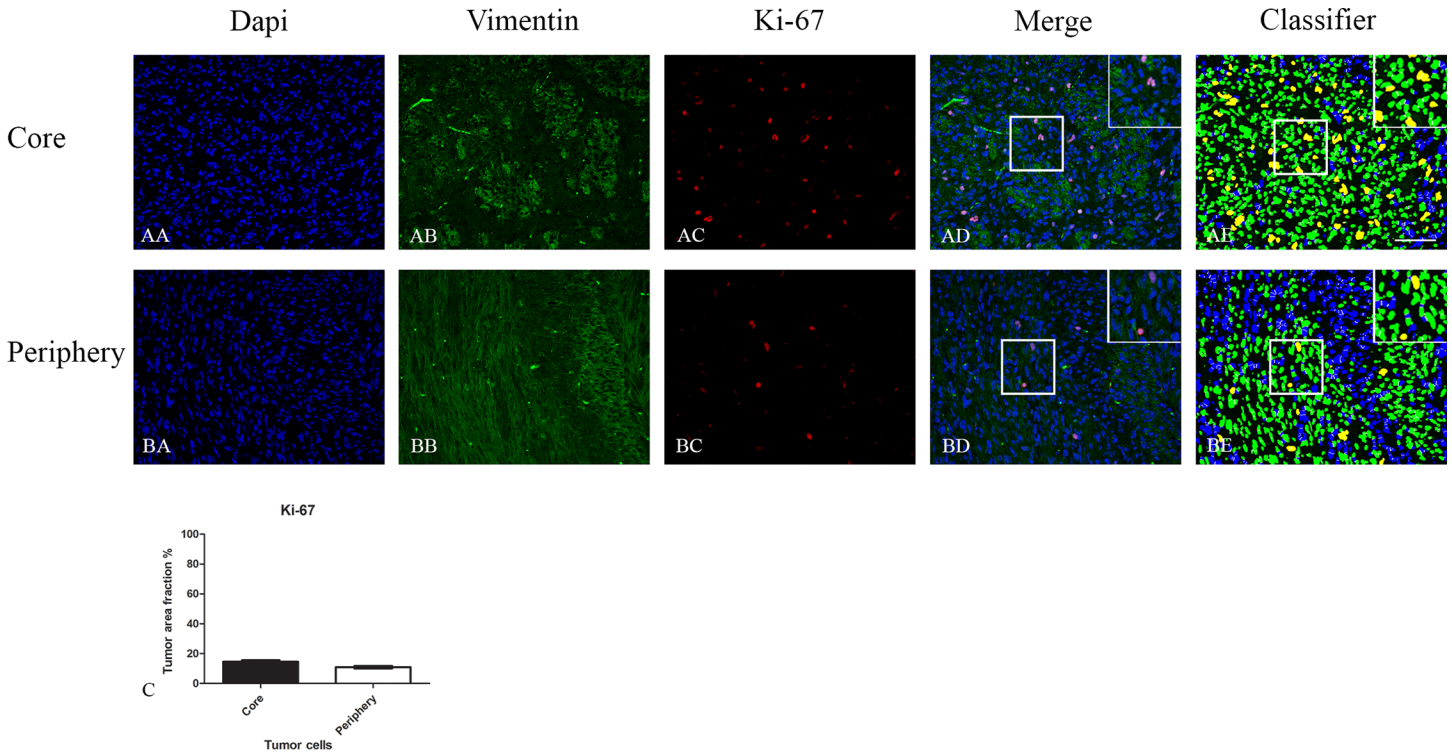

Fig 6. Double immunofluorescence staining of core and periphery in orthotopic model with five different patient derived GBM spheroid cultures. Tissues were stained with Dapi (blue), Vimentin (green) and Ki-67 (red). The software-based classifier is shown in the right column. The classifier illustrates tumor cells co-expressing markers of interest in yellow and tumor cells not co-expressing markers of interest in green. The fluorescence stainings were quantified in both core and periphery for Ki-67 (C). Statistical comparison was performed using student's t-test. Scalebar: 200μm.

doi:10.1371/journal.pone.0155106.g006

tumor aggressiveness–Ki-67 appeared to be expressed at similar levels in patient GBMs and GBM xenografts. The expression of Ki-67 in the GBM xenograft model showed a slightly reduced but not significant reduction in the periphery (n = 5), whereas the slightly reduced level was significant in patient GBMs (n = 26). In general, our results indicate that the orthotopic model to some degree mimics the migration scenario seen in patients Studies focusing on characteristics of migrating glioma cells and how they should be targeted could therefore to some extend be done in the orthotopic model.

In conclusion tumor cells in the periphery of patient gliomas have a stem cell phenotype, although it is less pronounced than in the tumor core. Novel therapies aiming at preventing recurrence should therefore take tumor stemness into account. In addition, known resistance factors like MGMT also seem to be preserved in the periphery of patient gliomas. Migrating cells in orthotopic glioblastoma xenografts preserve expression and stem cell markers. The orthotopic model therefore has a promising translational potential.

Supporting Information

S1 Fig. Double immunofluorescence staining of core and periphery of patient gliomas. Diffuse astrocytoma (AA-BE), oligo-astrocytoma (CA-DE), oligodendroglioma (EA-FE), anaplastic astrocytoma (GA-HE) and anaplastic oligo-astrocytoma (IA-JE) were stained with Dapi (blue), IDH1 (green) and Sox-2 (red). The software-based classifier is shown in the right column. The classifier illustrates tumor cells co-expressing Sox-2 in yellow and tumor cells not co-expressing Sox-2 in green. Scalebar: 200μm.
(TIF)

Acknowledgments

We would like to thank Helle Wohlleben and Tanja Dreehsen Højgaard for assistance with the immunohistochemical and fluorescence staining.

Author Contributions

Conceived and designed the experiments: SM FRP BWK. Performed the experiments: SM SAP. Analyzed the data: SM RHD BWK. Contributed reagents/materials/analysis tools: SM FRP BWK. Wrote the paper: SM SAP RHD FRP SH BWK.

References

1. Stupp R, Hegi ME, Mason WP, van den Bent MJ, Taphoorn MJ, Janzer RC, et al. Effects of radiotherapy with concomitant and adjuvant temozolomide versus radiotherapy alone on survival in glioblastoma in a randomised phase III study: 5-year analysis of the EORTC-NCIC trial. The lancet oncology. 2009; 10(5):459–66. Epub 2009/03/10. doi: 10.1016/s1470-2045(09)70025-7 PMID: 19269895.
2. Giese A, Westphal M. Glioma invasion in the central nervous system. Neurosurgery. 1996; 39(2):235–50; discussion 50–2. Epub 1996/08/01. PMID: 8832660.
3. Huang Z, Cheng L, Guryanova OA, Wu Q, Bao S. Cancer stem cells in glioblastoma—molecular signaling and therapeutic targeting. Protein & cell. 2010; 1(7):638–55. Epub 2011/01/05. doi: 10.1007/s13238-010-0078-y PMID: 21203936.
4. Singh SK, Hawkins C, Clarke ID, Squire JA, Bayani J, Hide T, et al. Identification of human brain tumour initiating cells. Nature. 2004; 432(7015):396–401. Epub 2004/11/19. doi: 10.1038/nature03128 PMID: 15549107.
5. Dean M, Fojo T, Bates S. Tumour stem cells and drug resistance. Nature reviews Cancer. 2005; 5 (4):275–84. Epub 2005/04/02. doi: 10.1038/nrc1590 PMID: 15803154.
6. Capper D, Zentgraf H, Balss J, Hartmann C, von Deimling A. Monoclonal antibody specific for IDH1 R132H mutation. Acta neuropathologica. 2009; 118(5):599–601. Epub 2009/10/03. doi: 10.1007/s00401-009-0595-z PMID: 19798509.

7. Capper D, Sahm F, Hartmann C, Meyermann R, von Deimling A, Schittenhelm J. Application of mutant IDH1 antibody to differentiate diffuse glioma from nonneoplastic central nervous system lesions and therapy-induced changes. The American journal of surgical pathology. 2010; 34(8):1199–204. Epub 2010/07/28. doi: 10.1097/PAS.0b013e3181e7740d PMID: 20661018.

8. von Deimling A, Korshunov A, Hartmann C. The next generation of glioma biomarkers: MGMT methylation, BRAF fusions and IDH1 mutations. Brain pathology (Zurich, Switzerland). 2011; 21(1):74–87. Epub 2010/12/07. doi: 10.1111/j.1750-3639.2010.00454.x PMID: 21129061.

9. Zheng PP, van der Weiden M, van der Spek PJ, Vincent AJ, Kros JM. Isocitrate dehydrogenase 1R132H mutation in microglia/macrophages in gliomas: Indication of a significant role of microglia/macrophages in glial tumorigenesis. Cancer Biology & Therapy. 2012; 13(10):836–9. doi: 10.4161/cbt.20836 PMID: 22785212; PubMed Central PMCID: PMCPmc3414408.

10. Joe YA, Hong YK, Chung DS, Yang YJ, Kang JK, Lee YS, et al. Inhibition of human malignant glioma growth in vivo by human recombinant plasminogen kringles 1–3. International journal of cancer Journal international du cancer. 1999; 82(5):694–9. Epub 1999/07/27. PMID: 10417767.

11. Huszthy PC, Daphu I, Niclou SP, Stieber D, Nigro JM, Sakariassen PO, et al. In vivo models of primary brain tumors: pitfalls and perspectives. Neuro-oncology. 2012; 14(8):979–93. Epub 2012/06/09. doi: 10.1093/neuonc/nos135 PMID: 22679124; PubMed Central PMCID: PMCPmc3408261.

12. Dahlrot RH, Hansen S, Herrstedt J, Schroder HD, Hjelmborg J, Kristensen BW. Prognostic value of Musashi-1 in gliomas. Journal of neuro-oncology. 2013; 115(3):453–61. Epub 2013/09/24. doi: 10.1007/s11060-013-1246-8 PMID: 24057325.

13. Hermansen SK, Kristensen BW. MicroRNA biomarkers in glioblastoma. Journal of neuro-oncology. 2013; 114(1):13–23. Epub 2013/05/24. doi: 10.1007/s11060-013-1155-x PMID: 23700324.

14. Corti S, Nizzardo M, Nardini M, Donadoni C, Locatelli F, Papadimitriou D, et al. Isolation and characterization of murine neural stem/progenitor cells based on Prominin-1 expression. Experimental neurology. 2007; 205(2):547–62. Epub 2007/05/01. doi: 10.1016/j.expneurol.2007.03.021 PMID: 17466977.

15. Lee A, Kessler JD, Read TA, Kaiser C, Corbeil D, Huttner WB, et al. Isolation of neural stem cells from the postnatal cerebellum. Nature neuroscience. 2005; 8(6):723–9. Epub 2005/05/24. doi: 10.1038/nn1473 PMID: 15908947; PubMed Central PMCID: PMCPmc2377345.

16. Uchida N, Buck DW, He D, Reitsma MJ, Masek M, Phan TV, et al. Direct isolation of human central nervous system stem cells. Proceedings of the National Academy of Sciences of the United States of America. 2000; 97(26):14720–5. Epub 2000/12/20. doi: 10.1073/pnas.97.26.14720 PMID: 11121071; PubMed Central PMCID: PMCPmc18985.

17. Singh SK, Clarke ID, Terasaki M, Bonn VE, Hawkins C, Squire J, et al. Identification of a cancer stem cell in human brain tumors. Cancer research. 2003; 63(18):5821–8. Epub 2003/10/03. PMID: 14522905.

18. Dahlrot RH, Hermansen SK, Hansen S, Kristensen BW. What is the clinical value of cancer stem cell markers in gliomas? International journal of clinical and experimental pathology. 2013; 6(3):334–48. Epub 2013/02/16. PMID: 23412423; PubMed Central PMCID: PMCPmc3563206.

19. Arai H, Ikota H, Sugawara K, Nobusawa S, Hirato J, Nakazato Y. Nestin expression in brain tumors: its utility for pathological diagnosis and correlation with the prognosis of high-grade gliomas. Brain tumor pathology. 2012; 29(3):160–7. Epub 2012/02/22. doi: 10.1007/s10014-012-0081-5 PMID: 22350668.

20. Dahlstrand J, Collins VP, Lendahl U. Expression of the class VI intermediate filament nestin in human central nervous system tumors. Cancer research. 1992; 52(19):5334–41. Epub 1992/10/01. PMID: 1382841.

21. Ehrmann J, Kolar Z, Mokry J. Nestin as a diagnostic and prognostic marker: immunohistochemical analysis of its expression in different tumours. Journal of clinical pathology. 2005; 58(2):222–3. Epub 2005/01/29. doi: 10.1136/jcp.2004.021238 PMID: 15677549; PubMed Central PMCID: PMCPmc1770570.

22. Kanamori M, Kumabe T, Sonoda Y, Nishino Y, Watanabe M, Tominaga T. Predictive factors for overall and progression-free survival, and dissemination in oligodendroglial tumors. Journal of neuro-oncology. 2009; 93(2):219–28. Epub 2008/12/23. doi: 10.1007/s11060-008-9762-7 PMID: 19099201.

23. Maderna E, Salmaggi A, Calatozzolo C, Limido L, Pollo B. Nestin, PDGFRbeta, CXCL12 and VEGF in glioma patients: different profiles of (pro-angiogenic) molecule expression are related with tumor grade and may provide prognostic information. Cancer Biology & Therapy. 2007; 6(7):1018–24. Epub 2007/07/06. PMID: 17611402.

24. Kim KJ, Lee KH, Kim HS, Moon KS, Jung TY, Jung S, et al. The presence of stem cell marker-expressing cells is not prognostically significant in glioblastomas. Neuropathology: official journal of the Japanese Society of Neuropathology. 2011; 31(5):494–502. Epub 2011/01/29. doi: 10.1111/j.1440-1789.2010.01194.x PMID: 21269333.

25. Kanemura Y, Mori K, Sakakibara S, Fujikawa H, Hayashi H, Nakano A, et al. Musashi1, an evolutionarily conserved neural RNA-binding protein, is a versatile marker of human glioma cells in determining their cellular origin, malignancy, and proliferative activity. Differentiation; research in biological diversity. 2001; 68(2–3):141–52. Epub 2001/11/01. PMID: 11686236.

26. Toda M, Iizuka Y, Yu W, Imai T, Ikeda E, Yoshida K, et al. Expression of the neural RNA-binding protein Musashi1 in human gliomas. Glia. 2001; 34(1):1–7. Epub 2001/04/03. PMID: 11284014.

27. Ma YH, Mentlein R, Knerlich F, Kruse ML, Mehdorn HM, Held-Feindt J. Expression of stem cell markers in human astrocytomas of different WHO grades. Journal of neuro-oncology. 2008; 86(1):31–45. Epub 2007/07/06. doi: 10.1007/s11060-007-9439-7 PMID: 17611714.

28. Strojnik T, Rosland GV, Sakariassen PO, Kavalar R, Lah T. Neural stem cell markers, nestin and musashi proteins, in the progression of human glioma: correlation of nestin with prognosis of patient survival. Surgical neurology. 2007; 68(2):133–43; discussion 43–4. Epub 2007/06/01. doi: 10.1016/j.surneu.2006.10.050 PMID: 17537489.

29. Phi JH, Park SH, Kim SK, Paek SH, Kim JH, Lee YJ, et al. Sox2 expression in brain tumors: a reflection of the neuroglial differentiation pathway. The American journal of surgical pathology. 2008; 32(1):103–12. Epub 2007/12/29. doi: 10.1097/PAS.0b013e31812f6ba6 PMID: 18162777.

30. Berezovsky AD, Poisson LM, Cherba D, Webb CP, Transou AD, Lemke NW, et al. Sox2 promotes malignancy in glioblastoma by regulating plasticity and astrocytic differentiation. Neoplasia. 2014; 16(3):193–206,.e19-25. Epub 2014/04/15. doi: 10.1016/j.neo.2014.03.006 PMID: 24726753; PubMed Central PMCID: PMCPmc4094829.

31. Tam WL, Ng HH. Sox2: masterminding the root of cancer. Cancer cell. 2014; 26(1):3–5. Epub 2014/07/16. doi: 10.1016/j.ccr.2014.06.024 PMID: 25026204.

32. Yan GN, Yang L, Lv YF, Shi Y, Shen LL, Yao XH, et al. Endothelial cells promote stem-like phenotype of glioma cells through activating the Hedgehog pathway. The Journal of pathology. 2014; 234(1):11–22. Epub 2014/03/08. doi: 10.1002/path.4349 PMID: 24604164; PubMed Central PMCID: PMCPmc4260128.

33. Dong Y, Han Q, Zou Y, Deng Z, Lu X, Wang X, et al. Long-term exposure to imatinib reduced cancer stem cell ability through induction of cell differentiation via activation of MAPK signaling in glioblastoma cells. Molecular and cellular biochemistry. 2012; 370(1–2):89–102. Epub 2012/07/26. doi: 10.1007/s11010-012-1401-0 PMID: 22829019.

34. Flavahan WA, Wu Q, Hitomi M, Rahim N, Kim Y, Sloan AE, et al. Brain tumor initiating cells adapt to restricted nutrition through preferential glucose uptake. Nature neuroscience. 2013; 16(10):1373–82. Epub 2013/09/03. doi: 10.1038/nn.3510 PMID: 23995067; PubMed Central PMCID: PMCPmc3930177.

35. Stupp R, Mason WP, van den Bent MJ, Weller M, Fisher B, Taphoorn MJ, et al. Radiotherapy plus concomitant and adjuvant temozolomide for glioblastoma. The New England journal of medicine. 2005; 352(10):987–96. Epub 2005/03/11. doi: 10.1056/NEJMoa043330 PMID: 15758009.

36. Sabit H, Nakada M, Furuta T, Watanabe T, Hayashi Y, Sato H, et al. Characterizing invading glioma cells based on IDH1-R132H and Ki-67 immunofluorescence. Brain tumor pathology. 2014. Epub 2014/01/05. doi: 10.1007/s10014-013-0172-y PMID: 24384677.

37. Louis DN, Ohgaki H, Wiestler OD, Cavenee WK, Burger PC, Jouvet A, et al. The 2007 WHO Classification of Tumours of the Central Nervous System. Acta neuropathologica. 2007; 114(2):97–109. doi: 10.1007/s00401-007-0243-4 PMID: 17618441; PubMed Central PMCID: PMCPmc1929165.

38. Jensen SS, Aaberg-Jessen C, Andersen C, Schroder HD, Kristensen BW. Glioma spheroids obtained via ultrasonic aspiration are viable and express stem cell markers: a new tissue resource for glioma research. Neurosurgery. 2013; 73(5):868–86; discussion 86. Epub 2013/07/28. doi: 10.1227/neu.0000000000000118 PMID: 23887192.

39. Cabrera MC, Hollingsworth RE, Hurt EM. Cancer stem cell plasticity and tumor hierarchy. World journal of stem cells. 2015; 7(1):27–36. doi: 10.4252/wjsc.v7.i1.27 PMID: 25621103; PubMed Central PMCID: PMCPMC4300934.

40. Bao S, Wu Q, McLendon RE, Hao Y, Shi Q, Hjelmeland AB, et al. Glioma stem cells promote radioresistance by preferential activation of the DNA damage response. Nature. 2006; 444(7120):756–60. Epub 2006/10/20. doi: 10.1038/nature05236 PMID: 17051156.

41. Eyupoglu IY, Buchfelder M, Savaskan NE. Surgical resection of malignant gliomas-role in optimizing patient outcome. Nature reviews Neurology. 2013; 9(3):141–51. Epub 2013/01/30. doi: 10.1038/nrneurol.2012.279 PMID: 23358480.

42. McGirt MJ, Chaichana KL, Attenello FJ, Weingart JD, Than K, Burger PC, et al. Extent of surgical resection is independently associated with survival in patients with hemispheric infiltrating low-grade gliomas. Neurosurgery. 2008; 63(4):700–7; author reply 7–8. doi: 10.1227/01.NEU.0000325729.41085.73 PMID: 18981880.

43. Zeppernick F, Ahmadi R, Campos B, Dictus C, Helmke BM, Becker N, et al. Stem cell marker CD133 affects clinical outcome in glioma patients. Clinical cancer research: an official journal of the American Association for Cancer Research. 2008; 14(1):123–9. doi: 10.1158/1078-0432.CCR-07-0932 PMID: 18172261.

44. Hermansen SK, Christensen KG, Jensen SS, Kristensen BW. Inconsistent immunohistochemical expression patterns of four different CD133 antibody clones in glioblastoma. The journal of histochemistry and cytochemistry: official journal of the Histochemistry Society. 2011; 59(4):391–407. Epub 2011/03/18. doi: 10.1369/0022155411400867 PMID: 21411810; PubMed Central PMCID: PMCPmc3201141.

45. Dahlrot RH, Hansen S, Jensen SS, Schroder HD, Hjelmborg J, Kristensen BW. Clinical value of CD133 and nestin in patients with glioma: a population-based study. International journal of clinical and experimental pathology. 2014; 7(7):3739–51. Epub 2014/08/15. PMID: 25120750; PubMed Central PMCID: PMCPmc4128985.

46. Christensen K, Schroder HD, Kristensen BW. CD133 identifies perivascular niches in grade II-IV astrocytomas. Journal of neuro-oncology. 2008; 90(2):157–70. Epub 2008/07/10. doi: 10.1007/s11060-008-9648-8 PMID: 18612800.

47. Lathia JD, Hitomi M, Gallagher J, Gadani SP, Adkins J, Vasanji A, et al. Distribution of CD133 reveals glioma stem cells self-renew through symmetric and asymmetric cell divisions. Cell death & disease. 2011; 2:e200. doi: 10.1038/cddis.2011.80 PMID: 21881602; PubMed Central PMCID: PMCPMC3186899.

48. Lind-Landstrom T, Varughese RK, Sundstrom S, Torp SH. Expression and clinical significance of the proliferation marker minichromosome maintenance protein 2 (Mcm2) in diffuse astrocytomas WHO grade II. Diagn Pathol. 2013; 8:67. doi: 10.1186/1746-1596-8-67 PMID: 23618321; PubMed Central PMCID: PMCPMC3648352.

49. Ambroise MM, Khosla C, Ghosh M, Mallikarjuna VS, Annapurneswari S. Practical value of MIB-1 index in predicting behavior of astrocytomas. Indian journal of pathology & microbiology. 2011; 54(3):520–5. doi: 10.4103/0377-4929.85085 PMID: 21934213.

50. Kolenda J, Jensen SS, Aaberg-Jessen C, Christensen K, Andersen C, Brunner N, et al. Effects of hypoxia on expression of a panel of stem cell and chemoresistance markers in glioblastoma-derived spheroids. Journal of neuro-oncology. 2011; 103(1):43–58. Epub 2010/09/14. doi: 10.1007/s11060-010-0357-8 PMID: 20835751.

51. Heddleston JM, Wu Q, Rivera M, Minhas S, Lathia JD, Sloan AE, et al. Hypoxia-induced mixed-lineage leukemia 1 regulates glioma stem cell tumorigenic potential. Cell Death Differ. 2012; 19(3):428–39. doi: 10.1038/cdd.2011.109 PMID: 21836617; PubMed Central PMCID: PMCPMC3229666.

52. Li Z, Bao S, Wu Q, Wang H, Eyler C, Sathornsumetee S, et al. Hypoxia-inducible factors regulate tumorigenic capacity of glioma stem cells. Cancer cell. 2009; 15(6):501–13. doi: 10.1016/j.ccr.2009.03.018 PMID: 19477429; PubMed Central PMCID: PMCPMC2693960.

53. Shin JH, Lee YS, Hong YK, Kang CS. Correlation between the prognostic value and the expression of the stem cell marker CD133 and isocitrate dehydrogenase1 in glioblastomas. Journal of neuro-oncology. 2013; 115(3):333–41. doi: 10.1007/s11060-013-1234-z PMID: 24129546.